Supplementary Materials of
Distributed Very Large Scale Bundle Adjustment by Global Camera Consensus

Runze Zhang
rzhangaj@cse.ust.hk

Siyu Zhu
szhu@cse.ust.hk

Tian Fang
fangtian@altizure.com

Long Quan
quan@cse.ust.hk

Department of Computer Science and Engineering
The Hong Kong University of Science and Technology

In the supplementary material, we first provide the convergence proof of ADMM algorithm on non-convex functions if the non-convex function satisfies some requirements. Then we will show information of the experiment data-sets, including selected input images, screenshots of distributed bundle adjustment results by our method and screenshots of selected blocks split by the proposed method.

1. Convergence Proof

We provide a proof for the following statement for non-convex function in this section and the convergence statement of ADMM algorithm for the bundle adjustment objective function in section 3.1 of the paper body can be obtained by using the following statement.

Theorem *With the objective function in Eqn. 7 in the paper body in which the gradients of each function f_i are local Lipschitz continuous with Lipschitz constant L_i, let $\{\mathbf{x}_i^t\} \subset \mathbb{R}^{nN}$ denote a sequence generated by the iterations in Eqn. 8, 9 and 10 in the paper body, where n is the dimension of variables and N is the number of split function. Then, there exists a $\rho > \max\{L_i, i = 1, ..., N\}$), such that the iterations in Eqn. 8, 9 and 10 in the paper body are guaranteed to converge to a local minimum of Eqn. 7 in the paper body.*

The convergence proof mainly refers to the convergence proof of ADMM on convex functions in the appendix of [2]. Note the right of Eqn. 8 in the paper body as $L_\rho^i(\mathbf{x}_i, \mathbf{z}, \mathbf{y}_i)$, namely

$$L_\rho^i(\mathbf{x}_i, \mathbf{z}, \mathbf{y}_i) = \left(f_i(\mathbf{x}_i) + \mathbf{y}_i^T(\mathbf{x}_i - \mathbf{z}) + \frac{\rho}{2}||\mathbf{x}_i - \mathbf{z}||_2^2\right) \quad \text{(S.1)}$$

The primal and dual residuals are

$$\begin{aligned} \mathbf{r}^t &= \left(\mathbf{r}_i^t, ..., \mathbf{r}_N^t\right) \\ \mathbf{s}^t &= -\rho \underbrace{\left(\mathbf{z}^t - \mathbf{z}^{k-1}, ..., \mathbf{z}^t - \mathbf{z}^{k-1}\right)}_{N} \end{aligned} \quad \text{(S.2)}$$

where $\mathbf{r}_i^t = \mathbf{x}_i^t - \mathbf{z}^t$.

Note $\mathbf{x}^t = (\mathbf{x}_1^t, ..., \mathbf{x}_N^t)$ and $\mathbf{y}^t = (\mathbf{y}_1^t, ..., \mathbf{y}_N^t)$. Let $(\mathbf{x}^*, \mathbf{z}^*, \mathbf{y}^*)$ be a saddle point for $\sum_{i=1}^N L_0^i(\mathbf{x}_i, \mathbf{z}, \mathbf{y}_i) = \sum_{i=1}(f_i(\mathbf{x}_i) + \mathbf{y}_i^T\mathbf{r}_i)$, where $\mathbf{x}^* = (\mathbf{x}_1^*, ..., \mathbf{x}_N^*)$ and $\mathbf{y}^* = (\mathbf{y}_1^*, ..., \mathbf{y}_N^*)$. Note p^* is the optimal value of Eqn. 7 in the paper body and $p^{t+1} = \sum_{i=1}^N f_i(\mathbf{x}_i^{t+1})$. Define

$$V^t = \frac{1}{\rho}\left\|\mathbf{y}^t - \mathbf{y}^*\right\|_2^2 + \rho N\left\|\mathbf{z}^t - \mathbf{z}^*\right\|_2^2 \quad \text{(S.3)}$$

The convergence proof of ADMM on convex functions contains three inequality

$$V^{t+1} \le V^t - \rho\left\|\mathbf{r}^{t+1}\right\|_2^2 - \rho N\left\|\mathbf{z}^{t+1} - \mathbf{z}^t\right\|_2^2 \quad \text{(S.4)}$$

$$\begin{aligned} p^{t+1} - p^* \le& -\mathbf{y}^{(t+1)T}\mathbf{r}^{t+1} \\ &- \rho\left(\mathbf{z}^{t+1} - \mathbf{z}^t\right)^T\left(N\left(\mathbf{z}^{t+1} - \mathbf{z}^*\right) + \sum_{i=1}^N \mathbf{r}_i^{t+1}\right) \end{aligned} \quad \text{(S.5)}$$

$$p^* - p^{t+1} \le \mathbf{y}^{*T}\mathbf{r}^{t+1} \quad \text{(S.6)}$$

Suppose above inequalities are satisfied, referring to [2], iterating the inequality S.4, we will get

$$\rho\sum_{t=0}^{\infty}\left(\left\|\mathbf{r}^{t+1}\right\|_2^2 + N\left\|\mathbf{z}^{t+1} - \mathbf{z}^t\right\|_2^2\right) \le V^0, \quad \text{(S.7)}$$

which implies that $\mathbf{r}^t \to 0$ and $\mathbf{z}^{t+1} - \mathbf{z}^t \to 0$ as $k \to 0$. $\mathbf{z}^{t+1} - \mathbf{z}^t \to 0$ means dual residual $\mathbf{s}^t \to 0$. $\mathbf{r}^t \to 0$ and $\mathbf{z}^{t+1} - \mathbf{z}^t \to 0$ results in that the right sides of inequalities S.5 and S.6 go to zero. Thus, we have $\lim_{t\to\infty} p^t = p^*$, namely the iteration will converge into the optimal value.

1.1. Proof of inequality S.6

Since $\mathbf{x}_i^* = \mathbf{z}^*$, we have

$$\sum L_0^i\left(\mathbf{x}_i^*, \mathbf{z}^*, \mathbf{y}_i^{*t}\right) = \sum f_i(\mathbf{x}_i^*) = p^*. \quad \text{(S.8)}$$

And

$$\sum L_0^i\left(\mathbf{x}_i^{t+1}, \mathbf{z}^{t+1}, \mathbf{y}_i^*\right) = p^{k+1} + \mathbf{y}^{*T}\mathbf{r}^{t+1}. \tag{S.9}$$

Since $(\mathbf{x}_i^*, \mathbf{z}^*, \mathbf{y}_i^*)$ is a saddle point for $\sum L_0^i$, we have $\sum L_0^i\left(\mathbf{x}_i^*, \mathbf{z}^*, \mathbf{y}_i^*\right) \leq \sum L_0^i\left(\mathbf{x}_i^{t+1}, \mathbf{z}^{t+1}, \mathbf{y}_i^*\right)$, namely,

$$p^* \leq p^{t+1} + \mathbf{y}^{*T}\mathbf{r}^{t+1}. \tag{S.10}$$

1.2. Proof of inequality S.5

In the proof of inequality S.5 in [2], L_ρ should be convex on the domain. However, if f is not convex, L_ρ cannot guarantee convex. Therefore, we need to show the convexity of L_ρ when the gradients of each function f_i are Lipschitz continuous with Lipschitz constant L_i.

Let's consider Eqn. 11 in the paper body in which $\mathbf{y}_i$ is substituted by $\rho\mathbf{u}_i$ from Eqn. 8 in the paper body. Let

$$\Psi_i(\mathbf{x}) = f_i(\mathbf{x}_i) + \frac{\rho}{2}\left\|\mathbf{x}_i - \mathbf{a}\right\|_2^2, \tag{S.11}$$

where $\mathbf{a} = \mathbf{z}^t - \mathbf{u}_i^t$. Then $\forall \mathbf{b}, \mathbf{c} \in \mathbb{R}^n$, we have

$$\begin{aligned}&\left(\nabla\Psi_i(\mathbf{b}) - \nabla\Psi_i(\mathbf{c})\right)^T(\mathbf{b}-\mathbf{c})\\ =&\left(\nabla f_i(\mathbf{b}) - \nabla f_i(\mathbf{c})\right)^T(\mathbf{b}-\mathbf{c}) + \rho\left\|\mathbf{b}-\mathbf{c}\right\|_2^2\end{aligned} \tag{S.12}$$

Since f_i is Lipschitz-continuous with a constant L_i, with Cauchy-Schwarz inequality, we have

$$\left(\nabla f_i(\mathbf{b}) - \nabla f_i(\mathbf{c})\right)^T(\mathbf{b}-\mathbf{c}) \geq -L_i\left\|\mathbf{b}-\mathbf{c}\right\|_2^2$$

Thus, we have

$$\left(\nabla\Psi_i(\mathbf{b}) - \nabla_i\Psi(\mathbf{c})\right)^T(\mathbf{b}-\mathbf{c}) \geq (\rho - L_i)\left\|\mathbf{b}-\mathbf{c}\right\|_2^2 \tag{S.13}$$

Since $\rho > \max\{L_i, i = 1, ..., N\}$, $\Psi(\mathbf{x}_i)$ is convex. Therefore, the optimality condition of Eqn. 11 in the paper body is

$$0 \in \nabla f_i\left(\mathbf{x}_i^{t+1}\right) + \rho\left(\mathbf{x}_i^{t+1} + \mathbf{u}_i^t - \mathbf{z}^t\right) \tag{S.14}$$

Substituting $\mathbf{u}_i^t = \frac{1}{\rho}\mathbf{y}_i^t$ and $\mathbf{y}_i^t = \mathbf{y}_i^{t+1} - \rho\mathbf{r}_i^{t+1}$, we have

$$0 \in \nabla f_i\left(\mathbf{x}_i^{t+1}\right) + \left(\mathbf{y}_i^{t+1} + \rho\left(\mathbf{z}^{t+1} - \mathbf{z}^t\right)\right) \tag{S.15}$$

Namely, for each $i = 1, ..., N$, $\mathbf{x}_i^{t+1}$ minimizes

$$f_i(\mathbf{x}) + \left(\mathbf{y}_i^{t+1} + \rho\left(\mathbf{z}^{t+1} - \mathbf{z}^t\right)\right)^T\mathbf{x}_i \tag{S.16}$$

Since each $\mathbf{x}_i$ is independent, accumulating all Eqn. S.16, we have that $\mathbf{x}^{t+1}$ minimizes

$$f(\mathbf{x}) + \sum_{i=1}^N\left(\mathbf{y}_i^{t+1} + \rho\left(\mathbf{z}^{t+1} - \mathbf{z}^t\right)\right)^T\mathbf{x}_i \tag{S.17}$$

Namely,

$$\begin{aligned}&f\left(\mathbf{x}^{t+1}\right) + \sum_{i=1}^N\left(\mathbf{y}_i^{t+1} + \rho\left(\mathbf{z}^{t+1} - \mathbf{z}^t\right)\right)^T\mathbf{x}_i^{t+1}\\ \leq& f\left(\mathbf{x}^*\right) + \sum_{i=1}^N\left(\mathbf{y}_i^{t+1} + \rho\left(\mathbf{z}^{t+1} - \mathbf{z}^t\right)\right)^T\mathbf{x}_i^*\end{aligned} \tag{S.18}$$

According to the consensus algorithm, $\mathbf{z}^{t+1}$ minimizes $L_\rho(\mathbf{x}^{t+1}, \mathbf{z}, \mathbf{y}^t)$, similar to above process, which implies $\mathbf{z}^{t+1}$ minimizes $-\sum_{i=1}^N \mathbf{y}_i^{(t+1)T}\mathbf{z}$, so we can get

$$-\sum_{i=1}^N\mathbf{y}_i^{(t+1)T}\mathbf{z}^{t+1} \leq -\sum_{i=1}^N\mathbf{y}_i^{(t+1)T}\mathbf{z}^* \tag{S.19}$$

Adding inequalities S.18 and S.19 and considering that $\mathbf{x}_i^* = \mathbf{z}$, after rearranging, we obtain the inequalities S.5.

1.3. Proof of inequality S.4

Referring to the appendix of [2], adding inequalities S.5 and S.6, regrouping terms, we can get

$$\begin{aligned}&2\left(\mathbf{y}^{t+1} - \mathbf{y}^*\right)^T\mathbf{r}^{t+1} + 2\rho\left(\mathbf{z}^{t+1} - \mathbf{z}^t\right)^T\sum_{i=1}^N\mathbf{r}_i^{t+1}\\ &+ 2\rho N\left(\mathbf{z}^{t+1} - \mathbf{z}^t\right)^T\left(\mathbf{z}^{t+1} - \mathbf{z}^*\right) \leq 0\end{aligned} \tag{S.20}$$

By using $\mathbf{y}^{t+1} = \mathbf{y}^t + \rho\mathbf{r}^{t+1}$ and rewriting terms, the above inequality can be written as

$$\begin{aligned}V^t - V^{t+1} \geq& \rho\left\|\mathbf{r}^{t+1}\right\|_2^2 + \rho N\left\|\mathbf{z}^{t+1} - \mathbf{z}^t\right\|_2^2\\ &+ 2\rho\left(\mathbf{z}^{t+1} - \mathbf{z}^t\right)^T\sum_{i=1}^N\mathbf{r}_i^{t+1}\end{aligned} \tag{S.21}$$

According to the consensus algorithm, similar to the process in section 1.2, $\mathbf{z}^{t+1}$ minimizes $-\sum_{i=1}^N\mathbf{y}_i^{(t+1)T}\mathbf{z}$ and $\mathbf{z}^t$ minimizes $-\sum_{i=1}^N\mathbf{y}_i^{tT}\mathbf{z}$, so

$$\begin{aligned}-\sum_{i=1}^N\mathbf{y}_i^{(t+1)T}\mathbf{z}^{t+1} &\leq -\sum_{i=1}^N\mathbf{y}_i^{(t+1)T}\mathbf{z}^t\\ -\sum_{i=1}^N\mathbf{y}_i^{tT}\mathbf{z}^t &\leq -\sum_{i=1}^N\mathbf{y}_i^{tT}\mathbf{z}^{t+1}\end{aligned} \tag{S.22}$$

Adding above inequality and substituting $\mathbf{y}_i^{t+1} - \mathbf{y}_i^t = \rho\mathbf{r}_i^{t+1}$, we have

$$\rho\left(\mathbf{z}^{t+1} - \mathbf{z}^t\right)^T\sum_{i=1}^N\mathbf{r}_i^{t+1} \geq 0. \tag{S.23}$$

Therefore, according inequality S.21,

$$V^t - V^{t+1} \geq \rho\left\|\mathbf{r}^{t+1}\right\|_2^2 + \rho N\left\|\mathbf{z}^{t+1} - \mathbf{z}^t\right\|_2^2 \tag{S.24}$$

Inequality S.4 is proved.

2. Experiment Data-set Information

In this section, we will provide some information of the experiment data-sets. Data-sets **LadyBug**, **Venice**, **Final 961** and **Final 13682** are obtained from the work [1] and this work only provides the SfM results of these data-sets without original images, so the points in the screenshots of SfM results are black. The blue rectangular pyramids are cameras, whose length of bottom side is proportional to image size and hight is proportional to the focal length. Since the input Structure-from-Motion results of **LadyBug**, **Venice**, **Final 961** and **Final 13682** provided by [1] are normalized, the principle points of cameras are $(0, 0)$. Besides, those data-sets do not have image sizes, so the cameras of those data-sets are visualized as blue lines before bundle adjustment. Since our distributed bundle adjustment method will refine principle points, the blue lines as cameras of those data-sets will change into pyramids with short bottom sides.

2.1. LadyBug

Figure. 1 shows the screenshots of SfM before and after distributed bundle adjustment by our method. The points after distributed bundle adjustment are more tidy. From Figure. 2, it is clear that principle points are adjusted in the bundle adjustment from zero to non-zero coordinates.

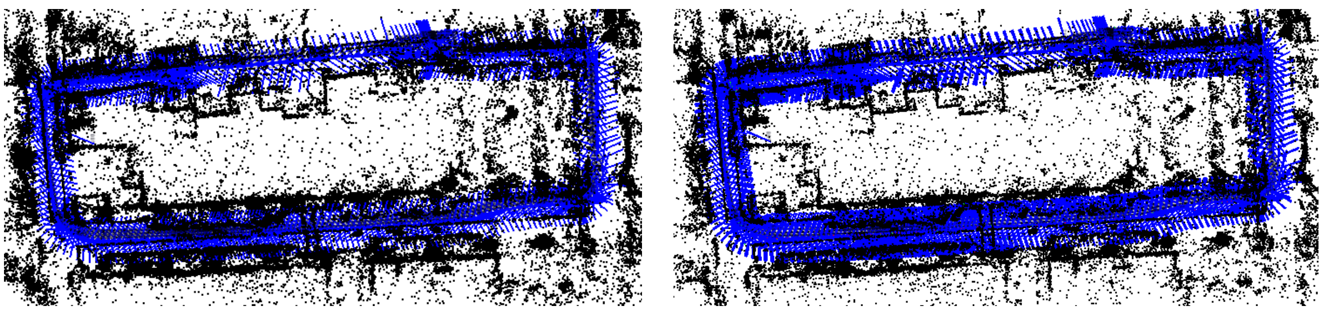

Figure 1: The screenshots of SfM for **LadyBug** before and after distributed bundle adjustment by our method. Left is before bundle adjustment and right is after bundle adjustment.

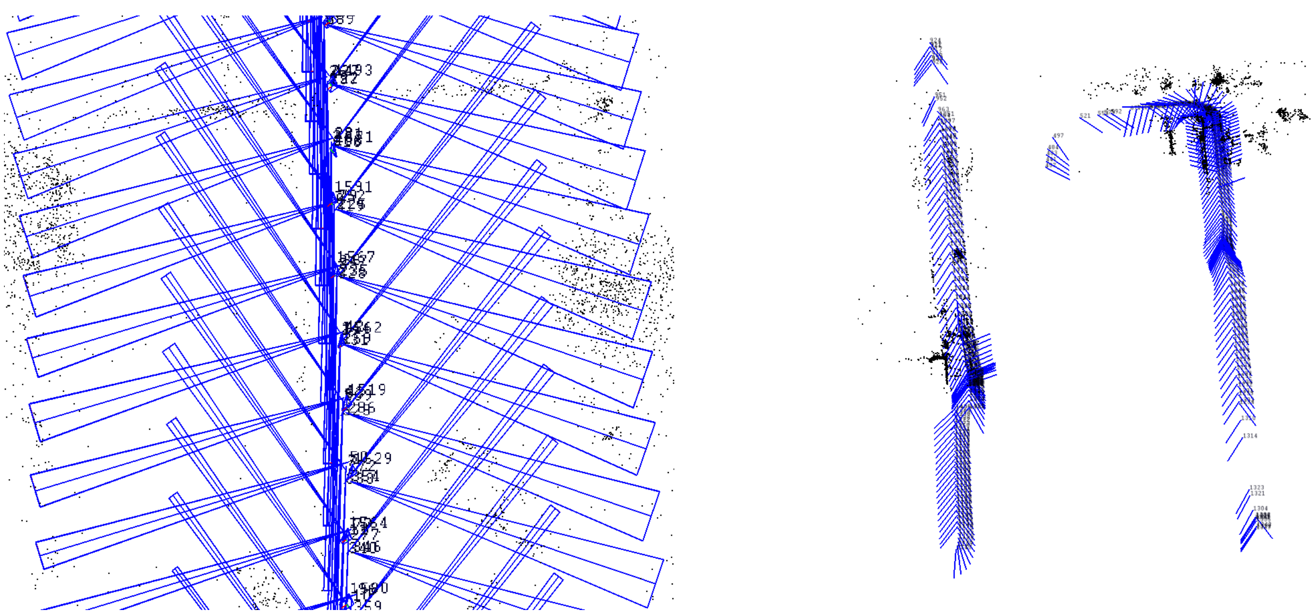

Figure 2: Left is the detail of distributed bundle adjustment result of **LadyBug**. Right is the screenshots of two blocks selected from all for **LadyBug** split by the proposed method.

2.2. Venice

The difference before and after bundle adjustment for **Venice** is not clear, so we only show the screenshot of the result after bundle adjustment in Figure. 3.

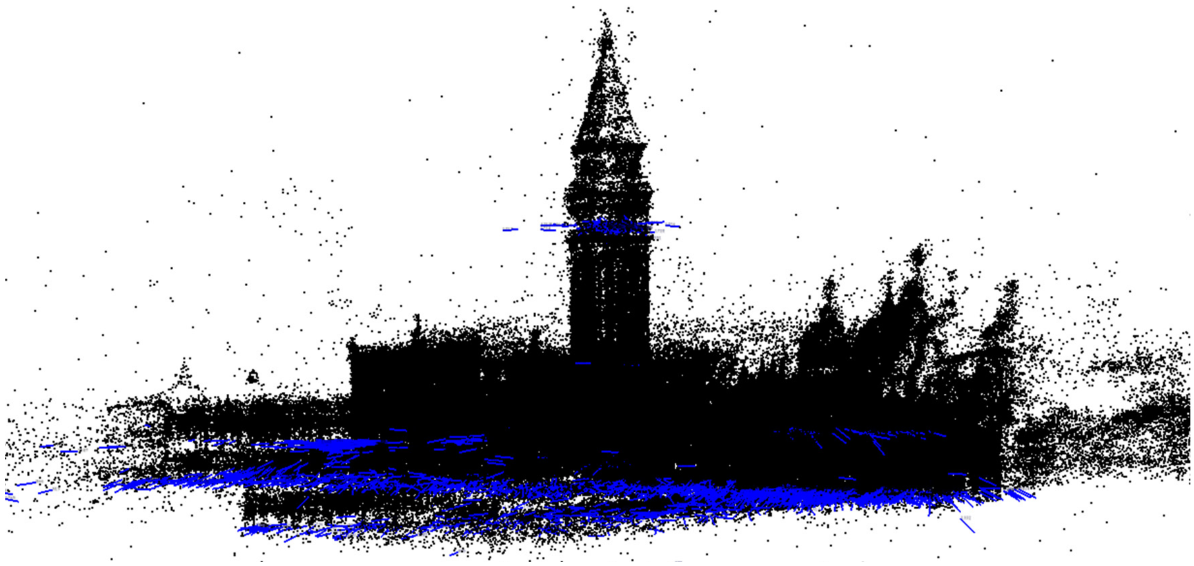

Figure 3: The screenshots of SfM for **Venice** after distributed bundle adjustment by our method.

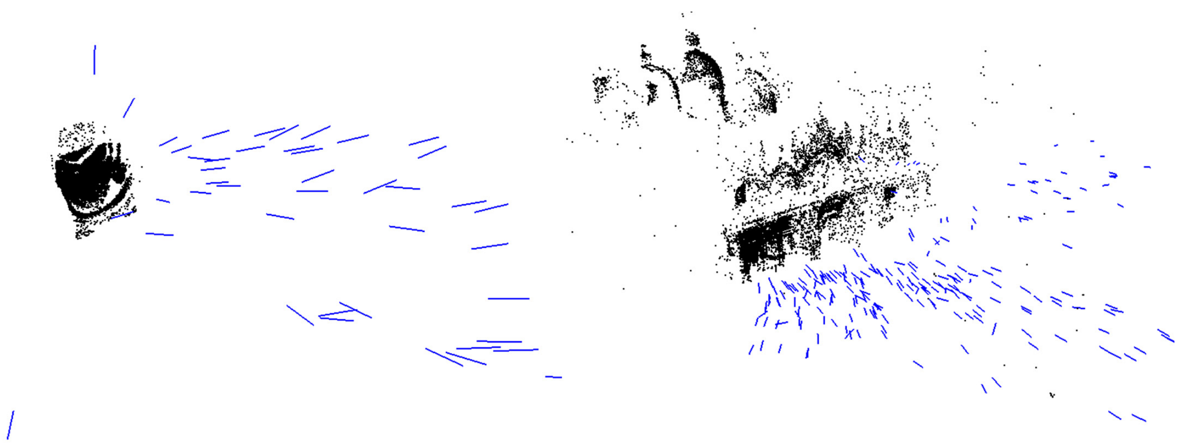

Figure 4: The screenshots of two blocks selected from all for **Venice** split by the proposed method.

2.3. Final 961

Figure. 5 shows the screenshots of SfM before and after distributed bundle adjustment by our method.

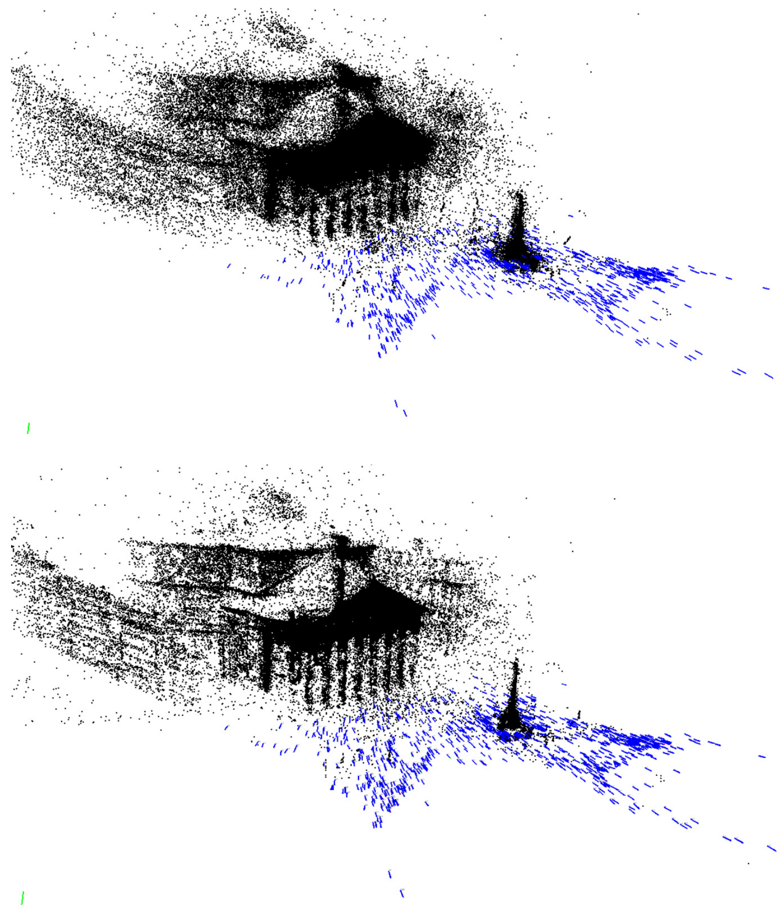

Figure 5: The screenshots of SfM for **Final 961** before and after distributed bundle adjustment by our method. Up is before bundle adjustment and down is after bundle adjustment.

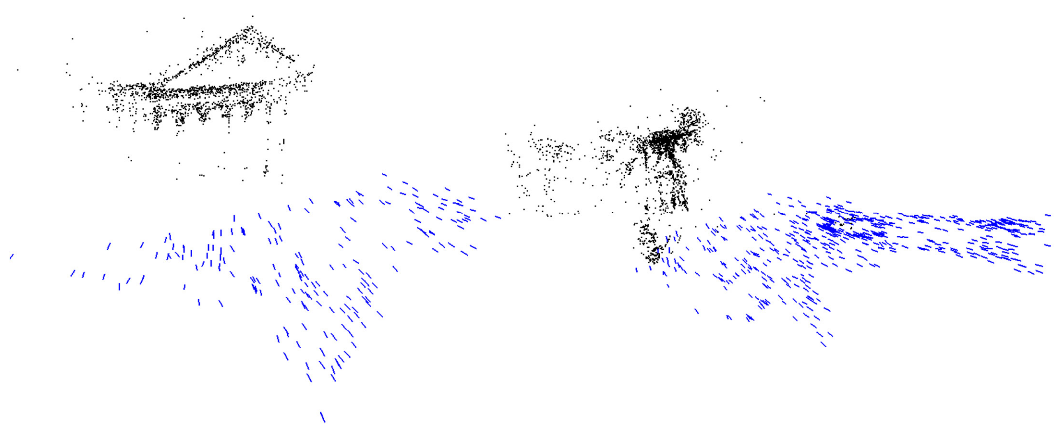

Figure 6: The screenshots of two blocks selected from all for **Final 961** split by the proposed method.

2.4. Final 13682

The difference before and after bundle adjustment for **Final 13682** is not clear, so we only show the screenshot of the result after bundle adjustment in Figure. 7.

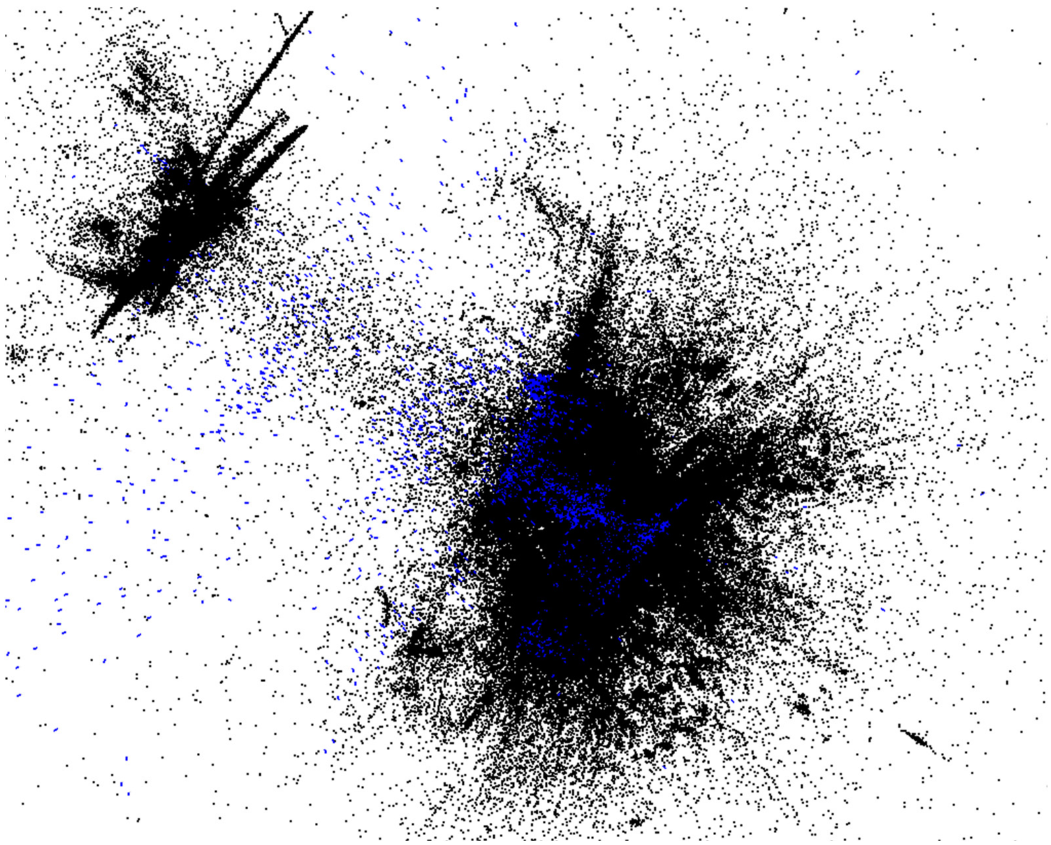

Figure 7: The screenshots of SfM for **Final 13682** after distributed bundle adjustment by our method.

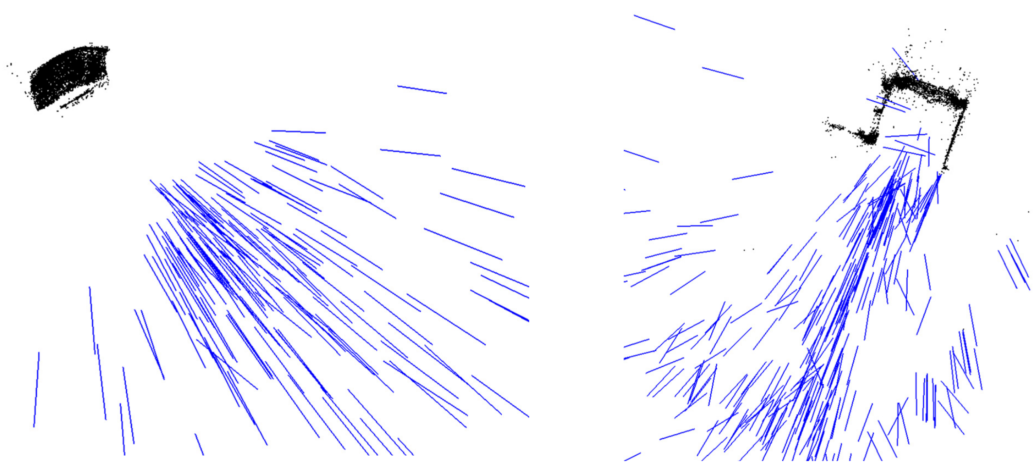

Figure 8: The screenshot of two blocks selected from all for **Final 13682** split by the proposed method.

2.5. Roman Forum

For the following data-sets, we will show some selected images. Since the difference of SfM results before and after bundle adjustment is not clear for the following data-sets, we only show the screenshots of results after bundle adjustment by our method.

Figure 9: Selected images of **Roman Forum**.

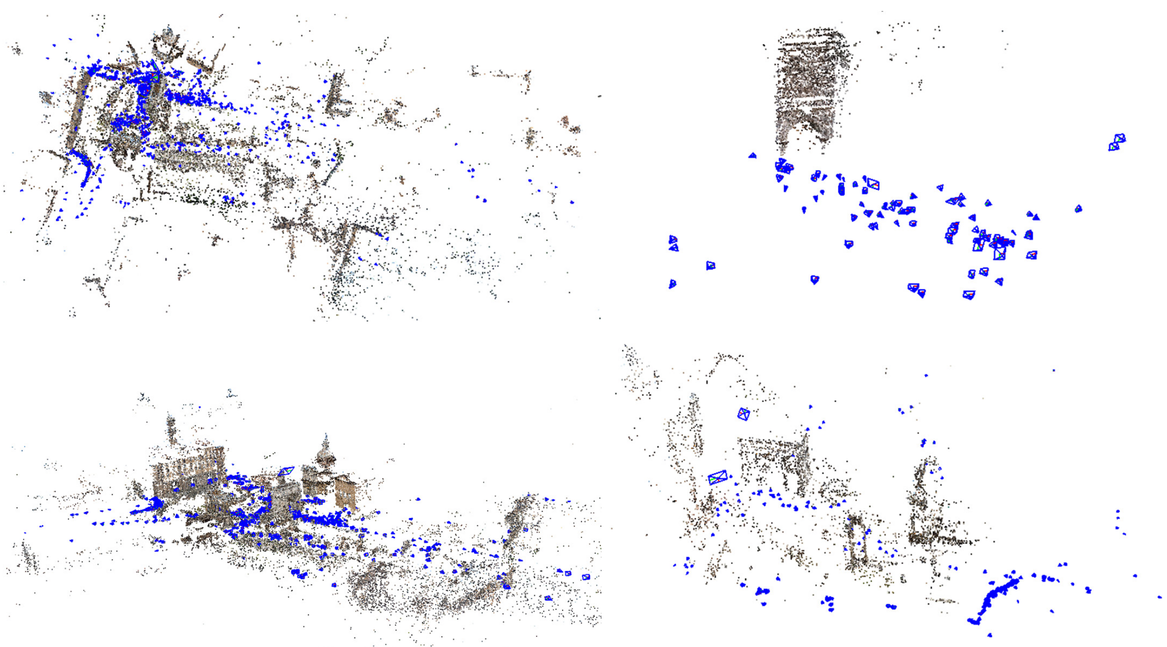

(a) (b)

Figure 10: (a) The screenshots of SfM for **Roman Forum** after distributed bundle adjustment by our method. Up is the top view and down is the perspective view. (b) The screenshots of two blocks selected from all for **Roman Forum** split by the proposed method.

2.6. Piccadilly

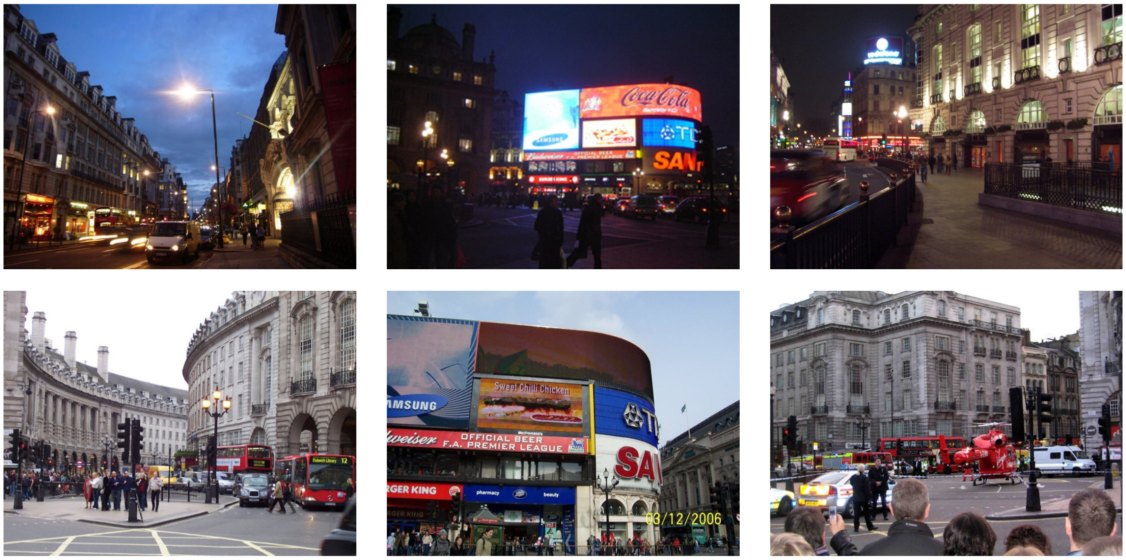

Figure 11: Selected images of **Piccadilly**.

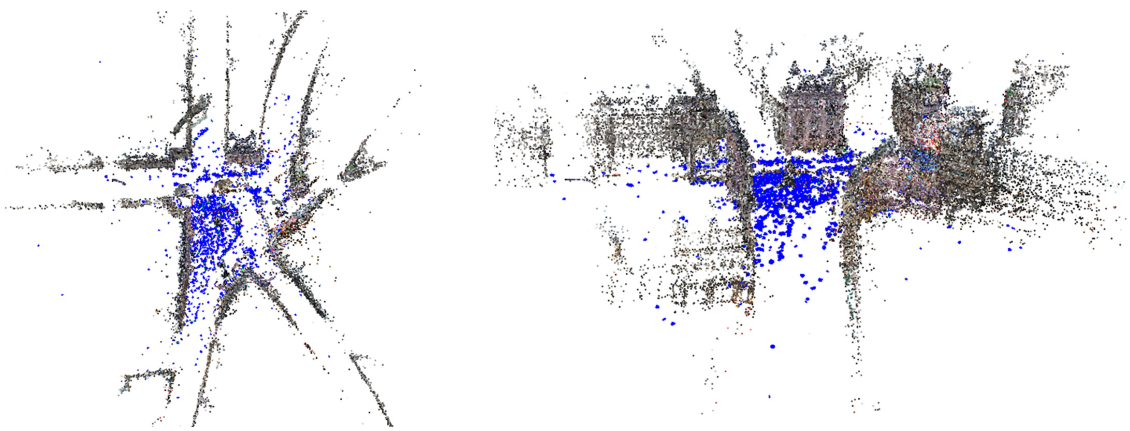

Figure 12: The screenshots of SfM for **Piccadilly** after distributed bundle adjustment by our method. Left is the top view and right is the perspective view.

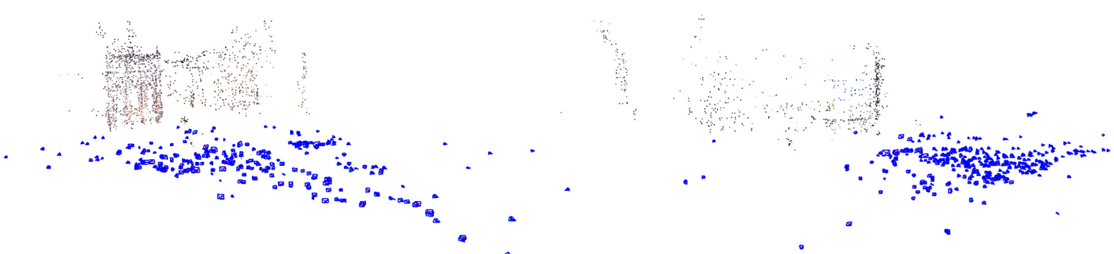

Figure 13: The screenshots of two blocks selected from all for **Piccadilly** split by the proposed method.

2.7. Trafalgar

Figure 14: Selected images of **Trafalgar**.

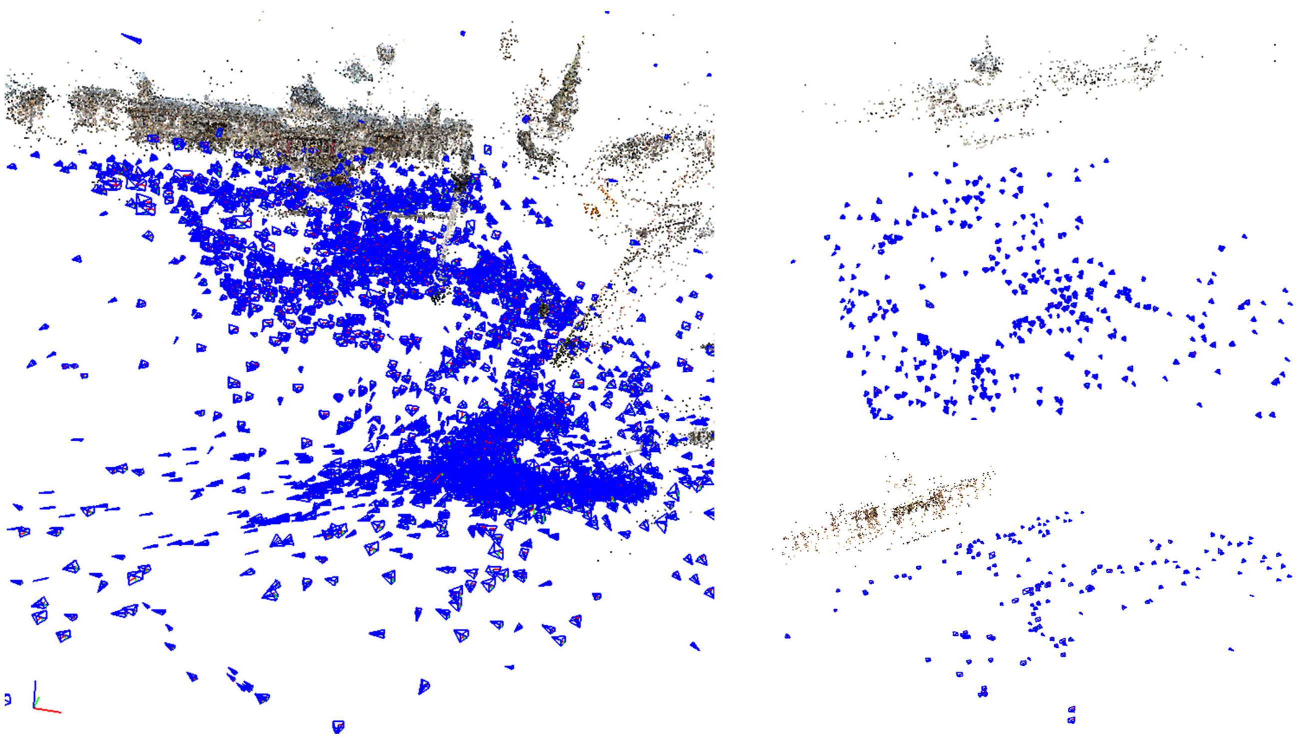

(a) (b)

Figure 15: (a) The screenshots of SfM for **Trafalgar** after distributed bundle adjustment by our method. (b) The screenshots of two blocks selected from all for **Trafalgar** split by the proposed method.

2.8. Buildings

Figure 16: Selected images of **Buildings**.

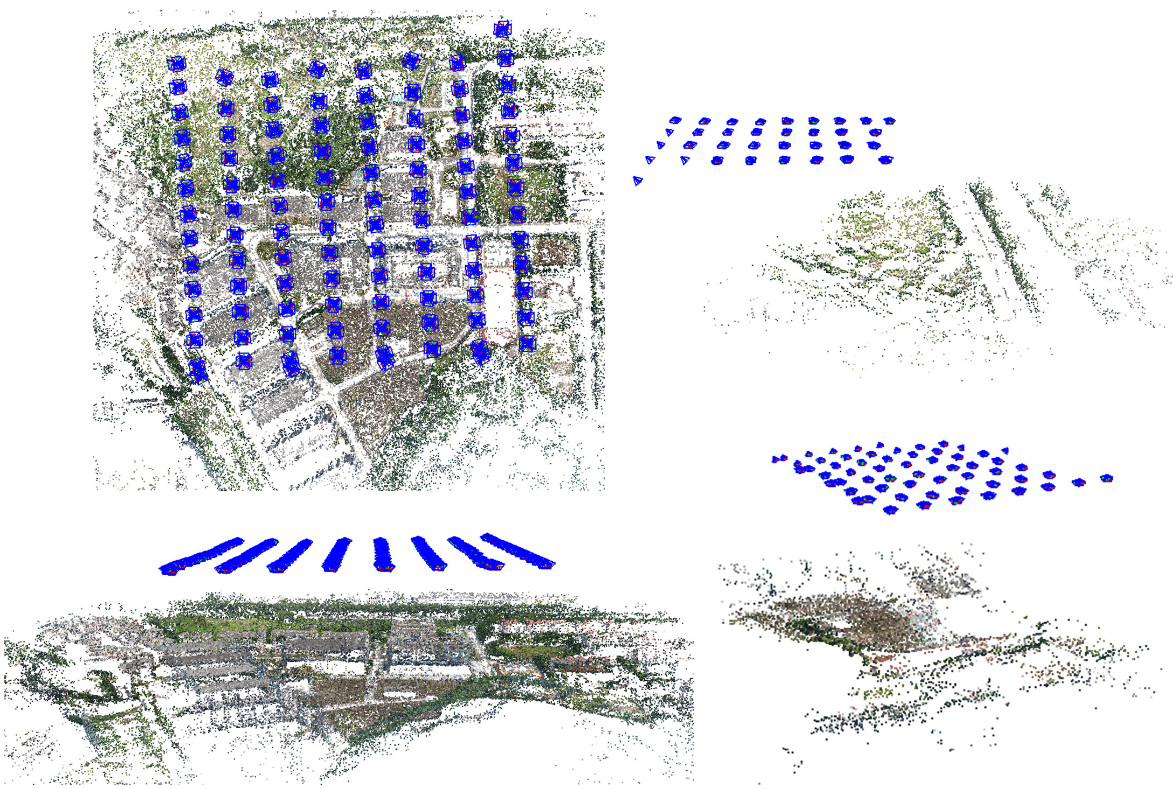

(a) (b)

Figure 17: (a) The screenshots of SfM for **Buildings** after distributed bundle adjustment by our method. Up is the top view and down is the perspective view. (b) The screenshots of two blocks selected from all for **Buildings** split by the proposed method.

2.9. Street

Figure 18: Selected images of **Street**.

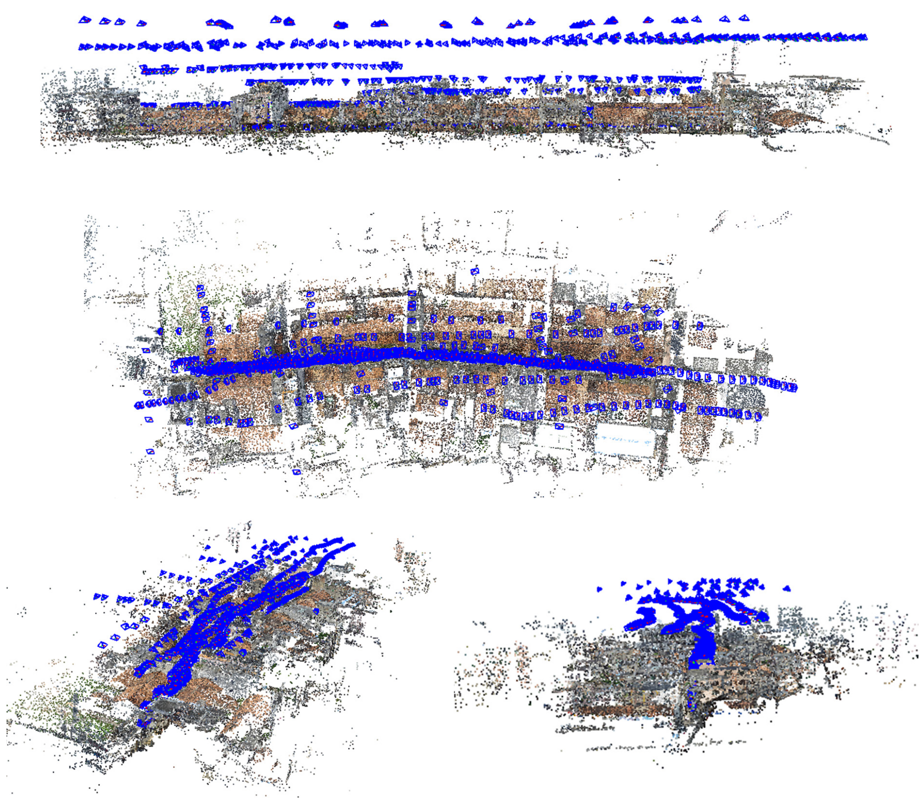

Figure 19: The screenshots of SfM for **Street** after distributed bundle adjustment by our method. Up is the side view, middle is the top view and the two in the bottom are the perspective view.

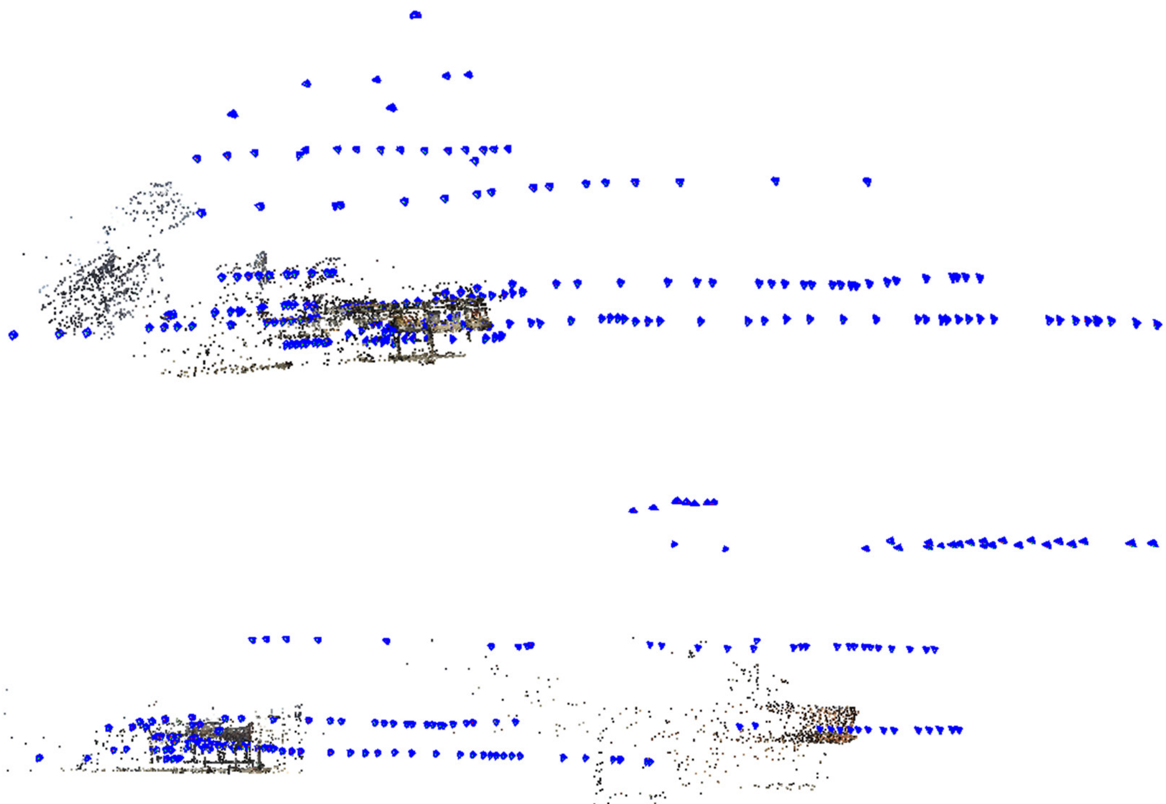

Figure 20: The screenshots of two blocks selected from all for **Street** split by the proposed method.

2.10. Town

Figure 21: Selected images of **Town**.

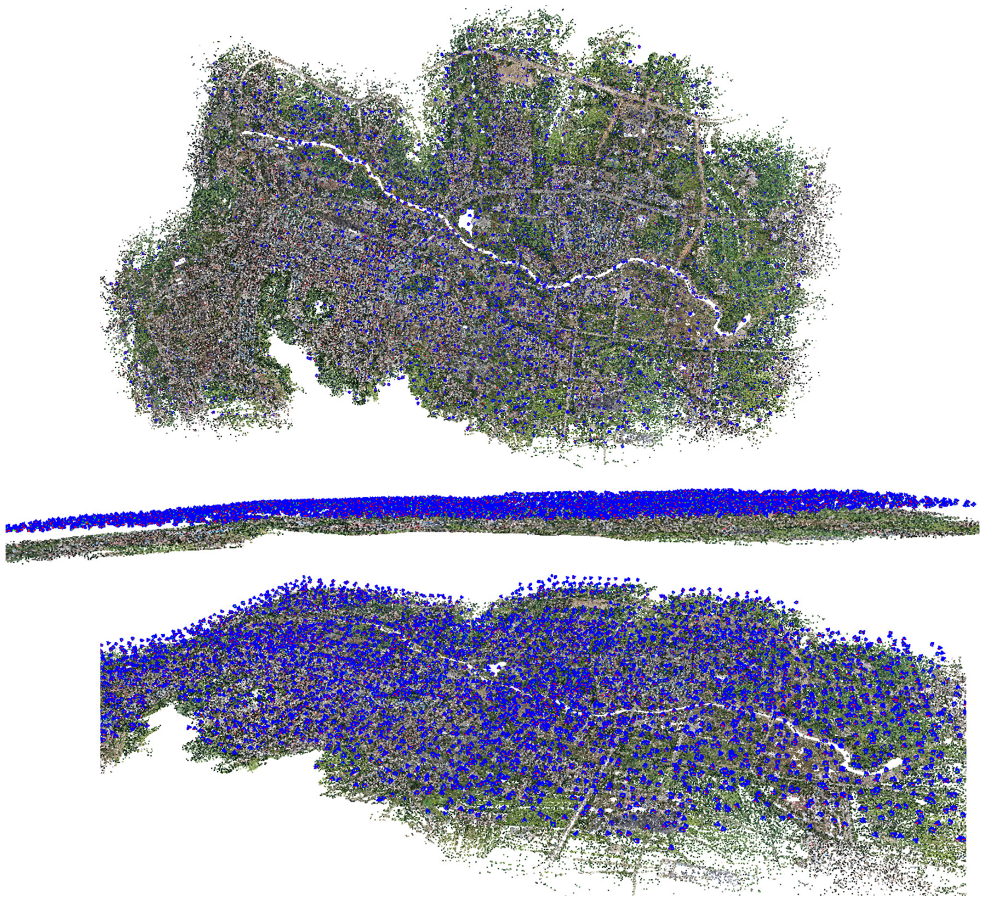

Figure 22: The screenshots of SfM for **Town** after distributed bundle adjustment by our method. Up is the top view, middle is the side view and bottom is the perspective view. Points are sampled for visualization.

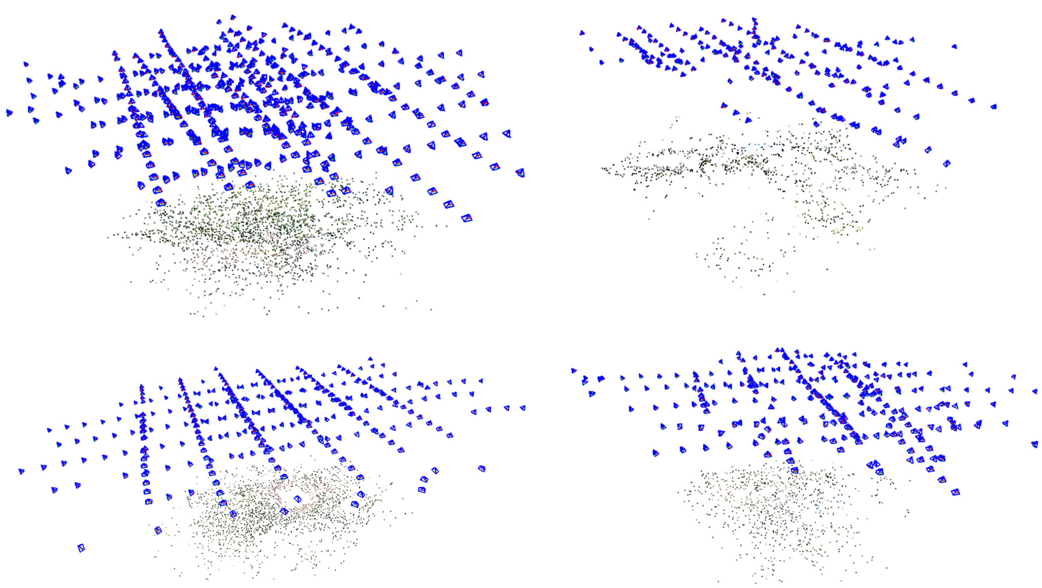

Figure 23: The screenshots of four blocks selected from all for **Town** split by the proposed method.

2.11. City

Figure 24: Selected images of **City**.

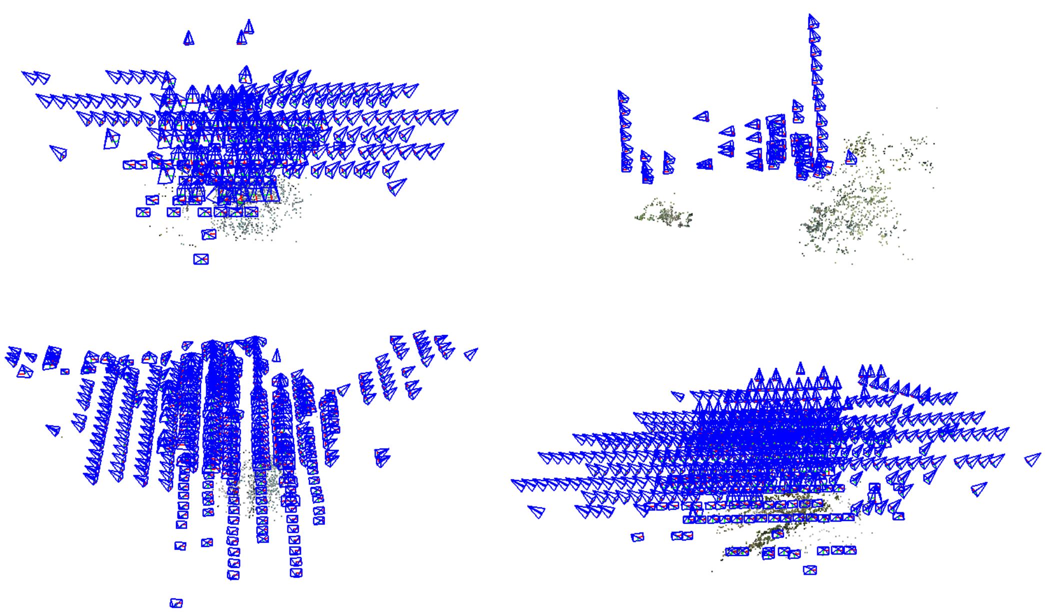

Figure 25: The screenshots of four blocks selected from all for **City** split by the proposed method.

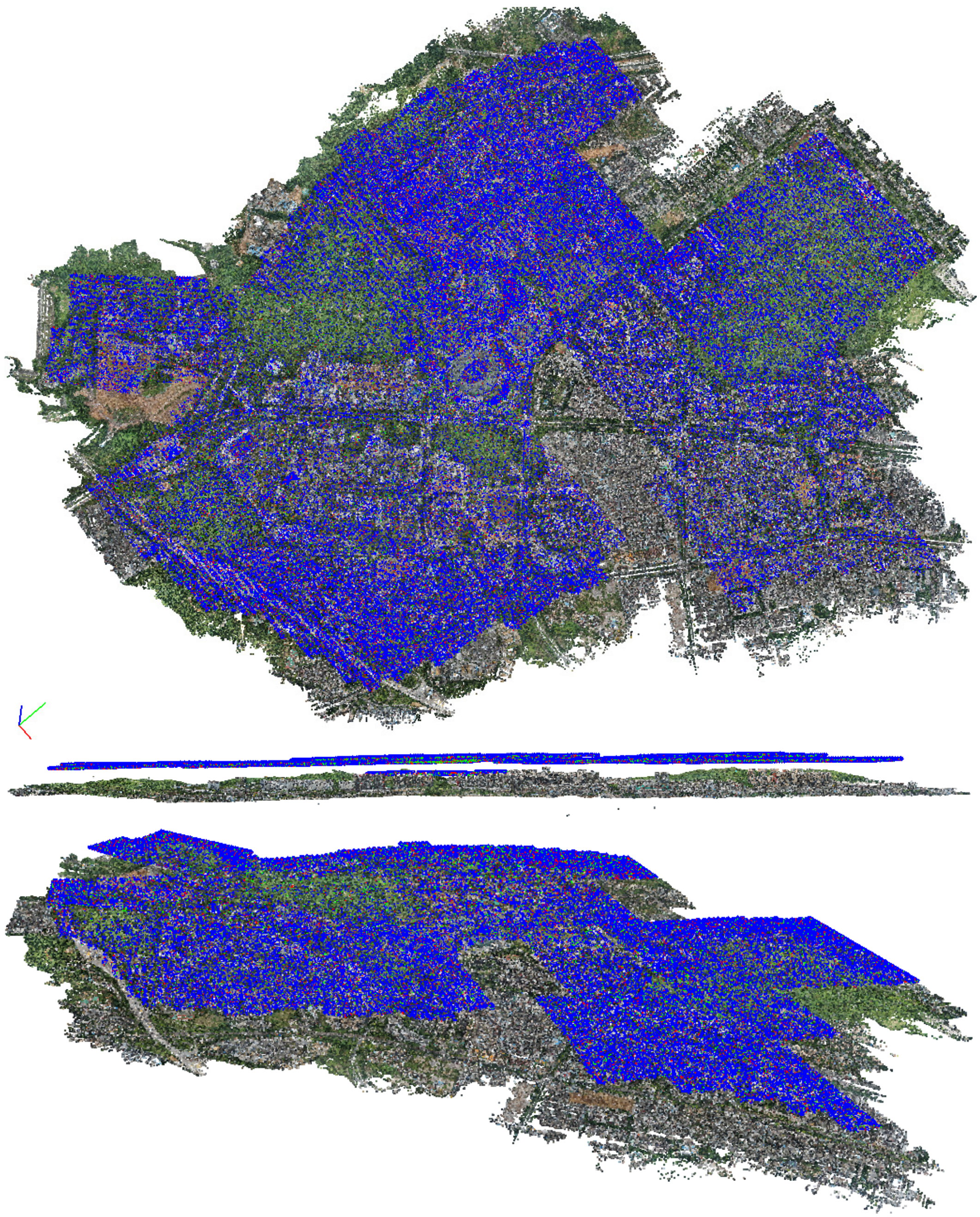

Figure 26: The screenshots of SfM for **City** after distributed bundle adjustment by our method. Up is the top view, middle is the side view and bottom is the perspective view. Points are sampled for visualization.

References

[1] S. Agarwal, N. Snavely, S. M. Seitz, and R. Szeliski. Bundle adjustment in the large. In *European Conference on Computer Vision*, pages 29–42. Springer, 2010.

[2] S. Boyd, N. Parikh, E. Chu, B. Peleato, and J. Eckstein. Distributed optimization and statistical learning via the alternating direction method of multipliers. *Foundations and Trends® in Machine Learning*, 3(1):1–122, 2011.